ChemComm

Intramolecular chalcogen bonding to tune the molecular conformation of helical building blocks for a supramolecular helix†

Peimin Weng, Xiaosheng Yan, [iD] *‡ Jinlian Cao, Zhao Li and Yun-Bao Jiang [iD] *

We propose to employ intramolecular chalcogen bonding to make a helical building block take its otherwise unfavorable *cis*-conformation. The 2,5-thiophenediamide motif was taken to bridge two β-turn structures to lead to an azapeptide that exists in *cis*-conformation and forms a halogen-bonded single-strand helix that exhibits a much stronger supramolecular helicity and a higher thermal stability.

As an emerging noncovalent interaction similar to hydrogen and halogen bonding, intermolecular chalcogen bonding[1] has recently been employed with great success in molecular recognition,[2] transmembrane transport,[3] catalysis[4] and supramolecular assembly.[5] In this context, we recently applied intermolecular S⋯S and S⋯O chalcogen bonding to derive supramolecular helices from alanine-based helical azapeptides containing a β-turn structure.[6] It was also noted that chalcogen bonding can function as an intramolecular interaction to maintain the specified molecular conformation.[7] For example, intramolecular S⋯O and S⋯N interactions have been utilized to lock the conformation of extended π-conjugated molecules, increasing their planarity and rigidity and thereby improving their electronic and physical properties.[8–10]

We therefore initiated our efforts to tune the molecular conformation of the helical building blocks expected to form supramolecular helices, by taking the intramolecular chalcogen bonding, using our previously established building block platform, azapeptide L,L-**AI** (Fig. 1a), which contains two terminal β-turn structures in the more stable and extended *trans*-conformation (Fig. 1a).[11] It was expected that if the molecule

could be made to exist in its *cis*-conformation, the resultant supramolecular helix would have a shorter pitch and likely enhanced characteristics in terms of, for example, helicity and stability.

To do that, the two carbonyl C=O bonds in the terephthalamide moiety in **AI** (Fig. 1a) should be forced to take that unfavorable mutual orientation. The phenyl ring was therefore replaced by a thiophene motif in order to employ the two S⋯O=C chalcogen bonds in the 2,5-thiophenediamide motif (Fig. 1b), to make the structurally symmetric **TAI** molecule into the *cis*-conformation. Meanwhile, the two chalcogen bonds would join the two ten-membered ring intramolecular hydrogen bonds that maintain the terminal β-turns to form a consecutive non-covalent bonding network within the folded **TAI** molecule (Fig. 1b), making the helical species more rigid, which
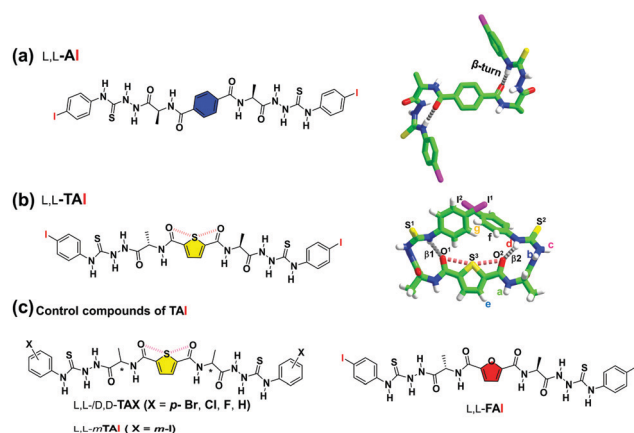

Fig. 1 (a) Molecular and crystal structures of L,L-**AI** that exists in *trans*-conformation. (b) Molecular and crystal structures of newly designed L,L-**TAI** that takes the *cis*-conformation because of the two intramolecular S⋯O=C chalcogen bonds. (c) Chemical structures of control compounds of **TAI**, L,L-/D,D-**TAX** (X = *p*-Br, Cl, F, H), L,L-*m***TAI** and L,L-**FAI**. The asterisks in the molecular structures indicate the chiral carbons, while the dashed grey and pink lines highlight the intramolecular hydrogen bonds and chalcogen bonds, respectively. For details of the synthesis of **TAI** and its control compounds, see procedures given in Schemes S1–S3, ESI.†

Department of Chemistry, College of Chemistry and Chemical Engineering, The MOE Key Laboratory of Spectrochemical Analysis and Instrumentation, and iChEM, Xiamen University, Xiamen 361005, China. E-mail: xshyan@xmu.edu.cn, ybjiang@xmu.edu.cn

‡ Present address: School of Pharmaceutical Sciences, Xiamen University, Xiamen 361102, China.

will also promote the assembling of them into a supramolecular helix.[12–14] Our experiments confirm that the newly developed building block molecule L,L- or D,D-**TAI** adopts the *cis*-conformation and forms a supramolecular single-strand *M*- or *P*-helix, respectively. The helix is of a much shorter pitch, almost half of that of **AI**, and exhibits a stronger helicity, together with a higher thermal stability in CH_3CN.

Calculations support that the **TAI** molecule prefers the *cis*-conformation with two intramolecular $S \cdots O = C$ chalcogen bonds and two β-turns (Fig. S1, ESI†). The structure of crystals of L,L-**TAI**, obtained from its solutions in 200 : 1 (v/v) $DMSO/H_2O$ (Table S1 and Fig. S2, ESI†), confirms that it takes the *cis*-conformation, with respect to the two terminal β-turns that are maintained by ten-membered ring hydrogen bonds (labelled as β1 and β2, Fig. 1b and Table S2, ESI†).[15,16] The $S^3 \cdots O^1$ and $S^3 \cdots O^2$ distances, measured as 2.977 Å and 2.920 Å, respectively, are both shorter than the sum of the van der Waals radii of O and S atoms (3.320 Å), suggesting that $S^3 \cdots O^1$ and $S^3 \cdots O^2$ chalcogen bonding occurs (Fig. 1b and Table S3, ESI†).[1] The angles of $C-S^3 \cdots O$ (144.8° for CS^3O^1, 145.0° for CS^3O^2) deviate from linearity, presumably due to the rigid structure of the 2,5-thiophenediamide motif and the existence of β-turns that, respectively, employ O^1 and O^2 atoms as hydrogen bond acceptors. We carried out natural bond orbital (NBO) analysis,[17] which indicates the presence of the $LP(O)-\sigma^*(S-C)$ orbital delocalization. This further confirms the chalcogen bonding, and the second-order perturbation energies for $S^3 \cdots O^1$ and $S^3 \cdots O^2$ interactions are calculated to be 3.09 and 4.26 kJ mol^{-1} (Table S4, ESI†).[7] These two $S \cdots O = C$ chalcogen bonds directly bring the two helical β-turns into a consecutive intramolecular hydrogen and chalcogen bonding network, the *cis*-**TAI** molecule being actually made into a full helical pitch (Fig. 1b and 3a). ^1H NMR spectra of **TAI** in $CD_3CN/DMSO$-d_6 at different temperatures reveal that the chemical shift of $-NH^d$ exhibits a much smaller value of the temperature coefficient (−2.85 ppb °C^{-1}, Fig. 2a). This means that $-NH^d$ participates in an intramolecular hydrogen bond, such as the ten-membered ring hydrogen bond within the β-turn structure indicated in the crystal structure (Fig. 1b). Meanwhile, $-NH^a$ is suggested to be not involved in an intramolecular hydrogen bond because its chemical shift exhibits a dramatic temperature-dependence (−10.52 ppb °C^{-1}, Fig. 2a).
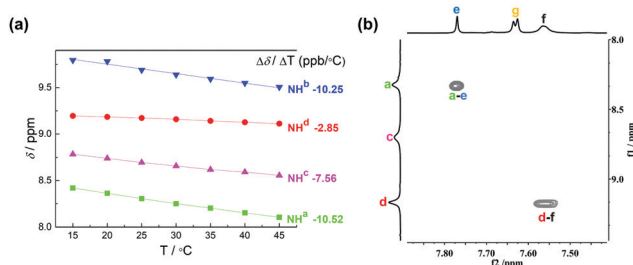
Together with the coupling between hydrogen atoms H^a and H^e observed in the 2D NOESY spectrum (Fig. 2b), **TAI** is confirmed to adopt its *cis*-conformation in the solution phase as well.

Detailed examination of the crystal structure indicates that L,L-**TAI** forms a single-strand supramolecular *M*-helix *via* intermolecular $C-I \cdots S$ halogen bonding interactions (Fig. 3).[18–21] Along the *b*-axis, two adjacent identical L,L-**TAI** molecules are bridged by one $C-I^2 \cdots S^1$ halogen bond (3.616 Å in $I^2 \cdots S^1$ distance, 170.5° and 78.0° in angles of $C-I^2 \cdots S^1$ and $I^2 \cdots S^1 = C$, respectively). This intermolecular $C-I \cdots S$ halogen bonding is essential, since control compounds **TAX** (X = Br, Cl, F, and H, Fig. 1c) with weaker or no halogen bonding ability,[22,23] do not form such supramolecular helices (Fig. S2–S4 and Tables S2, S3, ESI†). The helical pitch, 8.99 Å, is much shorter than that of the supramolecular helix from **AI**, 17.58 Å, in which a pitch consists of two **AI** molecules.[11] Enhancement in the helicity of the supramolecular helix of **TAI** is hence expected,[24–26] which will later be confirmed by its large *g*-factor (see Fig. 4c). The overall interaction energy in the $C-I^2 \cdots S^1$ halogen-bonded dimer of **TAI** is calculated to be −51.6 kJ mol^{-1} (Fig. S5, ESI†),[27,28] which is larger than that of the $C-I \cdots \pi$ halogen-bonded dimer in the **AI** helix (−40.6 kJ mol^{-1}).[11] NBO analysis reveals the occurrence of the intermolecular $LP(S^1)-\sigma^*(^2I-C)$ orbital delocalization, with a second-order perturbation energy of 3.17 kJ mol^{-1} (Table S4, ESI†), that supports the existence of the $C-I^2 \cdots S^1$ halogen bonding. The quantum theory of atoms in molecules (QTAIM)[29] was next employed to analyse the electron density and topology paths in the dimer of **TAI** (Fig. S6, ESI†), which indicates a strength of *ca.* −7.6 kJ mol^{-1} for the intermolecular local $C-I^2 \cdots S^1$ halogen bonding (Table S5, ESI†). Some other interactions, such as the van der Waals interactions (Table S6, ESI†), could also contribute to the overall interaction energy. The large overall interaction energy could be attributed to several factors existing in the **TAI** helix, a more efficient propagation of the helicity of the helical building block because of the much shorter pitch and the intramolecular
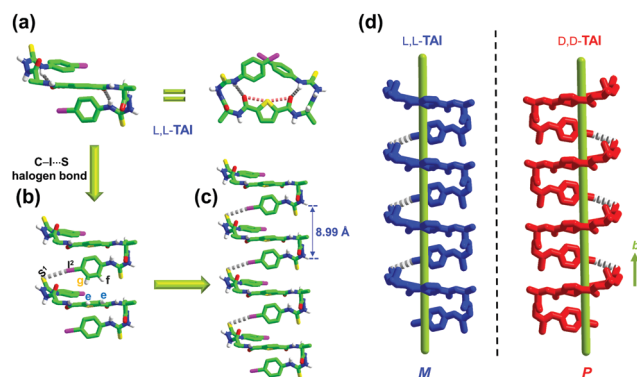

Fig. 2 (a) Influence on −NH resonances of L,L-**TAI** by temperature. Temperature coefficients are given by linear fitting of −NHs' chemical shifts. (b) Expanded 2D NOESY spectrum of **TAI** in DMSO-d_6/CD$_3$CN (5/95, v/v) (850 MHz, 25 °C, mixing time: 600 ms). [**TAI**] = 2 mM.

Fig. 3 (a) X-ray crystal structure of L,L-**TAI**. (b) $C-I^2 \cdots S^1$ halogen bond between two adjacent L,L-**TAI** molecules. (c and d) Single-stranded left-handed (*M*-) and right-handed (*P*-) supramolecular helices in the crystal packing of L,L-**TAI** and D,D-**TAI** molecules along the *b*-axis, respectively. Dashed dark grey lines, pink lines and grey lines represent hydrogen, chalcogen and $C-I \cdots S$ halogen bonds, respectively. For clarity, −CH hydrogen atoms are omitted.
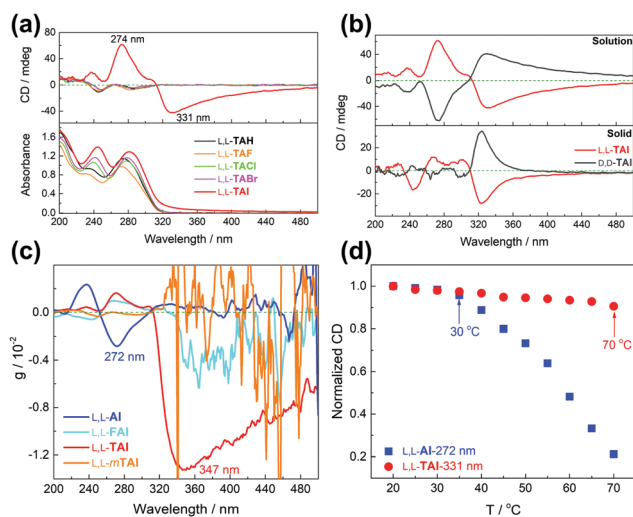
Fig. 4 (a) Absorption and CD spectra of L,L-**TAX** (X = H, F, Cl, Br, and I) in CH$_3$CN. [L,L-**TAX**] = 30 μM. (b) CD spectra of **TAI** in CH$_3$CN solution and in the solid state. The concentration of the solid samples is *ca.* 1 mg/60 mg KBr. (c) The *g* factor profiles of L,L-**AI**, L,L-**FAI**, L,L-**TAI** and L,L-*m***TAI**. [L,L-**AI**] = [L,L-**FAI**] = [L,L-**TAI**] = [L,L-*m***TAI**] = 30 μM. (d) The normalized CD intensities of L,L-**AI** at 272 nm and of L,L-**TAI** at 331 nm *versus* the temperature of the CH$_3$CN solution.

S···O═C chalcogen bonding and C═O···H–N hydrogen bonding network (with shared carbonyl O atom). D,D-**TAI** forms a supramolecular single-strand *P*-helix (Fig. 3d), as expected, mirror symmetric to that of L,L-**TAI**. This again confirms that the handedness of the supramolecular helix is determined by the molecular chirality of the alanine residues in the building block.

The supramolecular helix of **TAI** was shown to exist in solution as well. Compared to L,L-**TAX**s (X ≠ I), L,L-**TAI** in dilute CH$_3$CN solution exhibits red-shifted absorption and CD spectra, together with much stronger Cotton effects at 331 nm and 274 nm (Fig. 4a). These differences imply that supramolecular helical species may form from **TAI** in solution as well. The dynamic light scattering (DLS) profile of **TAI** in CH$_3$CN does show species of diameters around 180 nm, whereas **TAH**, **TAF**, **TACl** and **TABr** remain in their monomeric forms, showing DLS diameters around 4 nm (Fig. S7, ESI†). 1D and 2D NMR data also support the supramolecular helical structure of **TAI** in CH$_3$CN (Fig. S8, S9 and Table S7, ESI†), together with the observed intermolecular NOESY couplings of H^e–H^f and H^e–H^g (Fig. S9, ESI†).

CD spectral profiles of **TAI** in CH$_3$CN were found similar to those in the solid state (Fig. 4b), suggesting similar arrangements of **TAI** molecules in the solid state and in solution. For L,L-**TAI** in CH$_3$CN, the negative Cotton effect at longer wavelength of 331 nm suggests a left-handed helical conformation,[30,31] the same as that shown in the crystal structure (Fig. 3). Left- and right-handed helical fibers are observed in the SEM images of solution samples of L,L-**TAI** and D,D-**TAI** in CH$_3$CN, respectively (Fig. S10, ESI†), with a helical pitch of *ca.* 120 nm. AFM images of the solution samples of L,L-**TAI** in CH$_3$CN confirm the left-handed helical fibers, with

a height of *ca.* 11 nm (Fig. S10, ESI†). SEM images of the control compounds L,L-**TAX** (X ≠ I), however, show amorphous blocks (Fig. S11, ESI†).

It is worthy to point out that the control compound, L,L-**FAI** (Fig. 1c), containing a central 2,5-furandiamide motif without the illusive O···O═C chalcogen bonds, exists in a monomer form in CH$_3$CN, a conclusion made from its SEM image, DLS profile (Fig. S11 and S12, ESI†) and *g* factor (Fig. 4c). Despite its *cis*-conformation (Fig. S13, ESI†), the **FAI** molecule contains no consecutive interaction network and is thus of lower molecular rigidity, also seen from the broader NMR signals of –NHs in **FAI** (Fig. S14, ESI†). This strongly supports the function of the two S···O═C chalcogen bonds maintaining a consecutive intramolecular chalcogen and hydrogen bonding network in **TAI**, in promoting the formation of the supramolecular helix. The fact that another control compound containing a *meta*-I in the terminal phenyl ring, L,L-*m***TAI** (Fig. 1c), does not form a supramolecular helix in CH$_3$CN (Fig. 4c and Fig. S11, S12, ESI†) suggests that a well-matched intermolecular halogen bonding and intramolecular interaction network is required, which implies the cooperative nature of their functions in forming the helix so that the helicity of the building block is effectively propagated.

Finally, we found that the introduced S···O═C chalcogen bonds in the **TAI** molecule resulted in substantial enhancements of the characteristics of the supramolecular helix in CH$_3$CN. The CD intensities of L,L-**TAI** in CH$_3$CN depend on its concentration over 1–30 μM in a sigmoid manner, suggesting the cooperative nature of the intermolecular interactions during the formation of the supramolecular helix. The critical aggregation concentration of *ca.* 5 μM (Fig. S15, ESI†) is slightly lower than that of **AI** (*ca.* 6 μM).[11] CD profiles in terms of the anisotropic factor, *g*, point to an extremely high *g* factor of the **TAI** helix in CH$_3$CN, −1.35 × 10^{-2} (Fig. 4c), 5 times that of the helix of **AI** in CH$_3$CN (−0.28 × 10^{-2}) and almost 50 times that of the **TAI** monomer in a CH$_3$CN/H$_2$O mixture (−0.28 × 10^{-3}, Fig. S16, ESI†). This indicates a stronger helicity of the helix of **TAI**, which is now understandable in terms of the much shorter helical pitch of the supramolecular helix of **TAI**.[24–26] Regarding stability of the formed helix, we noted that the CD signals of **TAI** in CH$_3$CN remain almost unchanged upon heating up at least to 70 °C, whereas those of **AI** start to drop sharply beyond 35 °C (Fig. 4d). This means a much higher thermal stability of the supramolecular helix of **TAI** in CH$_3$CN (Fig. 4d and Fig. S17, S18, ESI†). CD spectra of L,L-**TAI** and L,L-**AI** in CH$_3$CN do not change after standing for 7 days, suggesting a high dynamic stability of the helix (Fig. S19, ESI†). A linear CD-ee-dependence was observed from the CD signals of the enantiomeric mixtures of **TAI** of various enantiomeric excess (ee) (Fig. S20 and S21, ESI†), meaning a self-sorting of **TAI** enantiomers in solution, likely resulting from the good propagation of the helicity of the helical building block.[32,33]

In summary, we introduced intramolecular chalcogen bonding interactions to control the molecular conformation and the intramolecular non-covalent interaction network of the helical building block for promoting its formation of a supramolecular

helix. The *N*-acylalanine-based amidothiourea motif that contains a β-turn structure was equipped into the 2,5-thiophenediamide linkage that provides with two S···O=C chalcogen bonds. The resultant building block **TAI** is therefore made to exist in the *cis*-conformation in terms of the two terminal β-turn structures that are included within the same intramolecular interaction network of the two N–H···O=C hydrogen bonds and two S···O=C chalcogen bonds. **TAI** self-assembles into a single-stranded supramolecular helix *via* a much stronger intermolecular single-point C–I···S halogen bonding, in both the solid state and dilute CH$_3$CN solution. The helix is of a much shorter pitch and exhibits a stronger helicity, with a *g*-factor of 0.014, and a higher thermal stability in CH$_3$CN. The CD-ee-dependence of the **TAI** helix in CH$_3$CN is almost linear, suggesting a self-sorting characteristic upon forming the supramolecular helix. A slight structural modification on the building block molecule is thus shown to exert a substantial impact on the formed supramolecular helix, demonstrating the great potential of using the intramolecular chalcogen bonding in tuning the molecular conformation and consequently the supramolecular assembly, to lead to structurally and functionally diverse smart materials.

Conflicts of interest

There are no conflicts of interest to declare.

Notes and references

1 C. B. Aakeroy, D. L. Bryce, G. R. Desiraju, A. Frontera, A. C. Legon, F. Nicotra, K. Rissanen, S. Scheiner, G. Terraneo, P. Metrangolo and G. Resnati, *Pure Appl. Chem.*, 2019, **91**, 1889–1892.
2 J. Y. Lim, I. Marques, A. L. Thompson, K. E. Christensen, V. Felix and P. D. Beer, *J. Am. Chem. Soc.*, 2017, **139**, 3122–3133.
3 S. Benz, M. Macchione, Q. Verolet, J. Mareda, N. Sakai and S. Matile, *J. Am. Chem. Soc.*, 2016, **138**, 9093–9096.
4 S. Benz, J. López-Andarias, J. Mareda, N. Sakai and S. Matile, *Angew. Chem.*, 2017, **129**, 830–833.
5 L. Chen, J. Xiang, Y. Zhao and Q. Yan, *J. Am. Chem. Soc.*, 2018, **140**, 7079–7082.
6 D. Shi, J. Cao, P. Weng, X. Yan, Z. Li and Y. B. Jiang, *Org. Biomol. Chem.*, 2021, **19**, 6397–6401.
7 D. J. Pascoe, K. B. Ling and S. L. Cockroft, *J. Am. Chem. Soc.*, 2017, **139**, 15160–15167.
8 H. Huang, L. Yang, A. Facchetti and T. J. Marks, *Chem. Rev.*, 2017, **117**, 10291–10318.
9 Y. Nagao, T. Hirata, S. Goto, S. Sano, A. Kakehi, K. Iizuka and M. Shiro, *J. Am. Chem. Soc.*, 1998, **120**, 3104–3110.
10 K. Hayashi, S. Ogawa, S. Sano, M. Shiro, K. Yamaguchi, Y. Sei and Y. Nagao, *Chem. Pharm. Bull.*, 2008, **56**, 802–806.
11 J. Cao, X. Yan, W. He, X. Li, Z. Li, Y. Mo, M. Liu and Y.-B. Jiang, *J. Am. Chem. Soc.*, 2017, **139**, 6605–6610.
12 S. Mondal, L. Adler-Abramovich, A. Lampel, Y. Bram, S. Lipstman and E. Gazit, *Nat. Commun.*, 2015, **6**, 8615.
13 R. Misra, A. Saseendran, S. Dey and H. N. Gopi, *Angew. Chem., Int. Ed.*, 2019, **58**, 2251–2255.
14 T. Sawada and M. Fujita, *Chem*, 2020, **6**, 1861–1876.
15 X. S. Yan, K. Wu, Y. Yuan, Y. Zhan, J. H. Wang, Z. Li and Y. B. Jiang, *Chem. Commun.*, 2013, **49**, 8943–8945.
16 X.-S. Yan, H. Luo, K.-S. Zou, J.-L. Cao, Z. Li and Y.-B. Jiang, *ACS Omega*, 2018, **3**, 4786–4790.
17 A. E. Reed, L. A. Curtiss and F. Weinhold, *Chem. Rev.*, 1988, **88**, 899–926.
18 X. Yan, K. Zou, J. Cao, X. Li, Z. Zhao, Z. Li, A. Wu, W. Liang, Y. Mo and Y. Jiang, *Nat. Commun.*, 2019, **10**, 3610.
19 C. Z. Liu, S. Koppireddi, H. Wang, D. W. Zhang and Z. T. Li, *Angew. Chem., Int. Ed.*, 2019, **58**, 226–230.
20 A. Vanderkooy, A. K. Gupta, T. Földes, S. Lindblad, A. Orthaber, I. Pápai and M. Erdélyi, *Angew. Chem., Int. Ed.*, 2019, **58**, 9012–9016.
21 Y. Xu, A. Hao and P. Xing, *Angew. Chem., Int. Ed.*, 2022, **61**, e202113786.
22 L. C. Gilday, S. W. Robinson, T. A. Barendt, M. J. Langton, B. R. Mullaney and P. D. Beer, *Chem. Rev.*, 2015, **115**, 7118–7195.
23 G. Cavallo, P. Metrangolo, R. Milani, T. Pilati, A. Priimagi, G. Resnati and G. Terraneo, *Chem. Rev.*, 2016, **116**, 2478–2601.
24 M. Xu, L. Liu and Q. Yan, *Angew. Chem., Int. Ed.*, 2018, **57**, 5029–5032.
25 A. Khan and S. Hecht, *Chem. – Eur. J.*, 2006, **12**, 4764–4774.
26 H. Sogawa, M. Shiotsuki and F. Sanda, *Macromolecules*, 2013, **46**, 4378–4387.
27 P. Deepa, B. V. Pandiyan, P. Kolandaivel and P. Hobza, *Phys. Chem. Chem. Phys.*, 2014, **16**, 2038–2047.
28 Y. Le Gal, D. Lorcy, O. Jeannin, F. Barrière, V. Dorcet, J. Lieffrig and M. Fourmigué, *CrystEngComm*, 2016, **18**, 5474–5481.
29 R. F. Bader, *Chem. Rev.*, 1991, **91**, 893–928.
30 C. C. Lee, C. Grenier, E. W. Meijer and A. P. Schenning, *Chem. Soc. Rev.*, 2009, **38**, 671–683.
31 G. Pescitelli, L. Di Bari and N. Berova, *Chem. Soc. Rev.*, 2014, **43**, 5211–5233.
32 X. Yan, Q. Wang, X. Chen and Y. B. Jiang, *Adv. Mater.*, 2020, **32**, 1905667.
33 C. Roche, H. J. Sun, M. E. Prendergast, P. Leowanawat, B. E. Partridge, P. A. Heiney, F. Araoka, R. Graf, H. W. Spiess, X. Zeng, G. Ungar and V. Percec, *J. Am. Chem. Soc.*, 2014, **136**, 7169–7185.